OPEN ACCESS
Journal of Multidisciplinary Applied Natural Science Vol. xx No. xx (xxxx) https://doi.org/10.47352/jmans.2774-3047.291
Check for updates
Research Article

Visibility, Selectivity, Optimization, and Interaction of Natural Tannin Dye from *Ceriops tagal* (Perr.) C.B. Rob. Extract for Plant Tissue Staining

Rasuane Noor, Maryani Maryani*, Bambang Retnoaji, and Edia Rahayuningsih

Received : May 23, 2025	Revised : June 27, 2025	Accepted : June 29, 2025	Online : August 09, 2025

Abstract
Tissue staining improves cellular visualization for microscopic analysis. This study explores tannin dye from *Ceriops tagal* as a sustainable, eco-friendly alternative for plant histology. Its strong affinity to cotton cellulose suggests effective staining potential. The research assesses tissue visibility, mordant specificity, color contrast, and dye–tissue binding interactions. Tissue staining enhances the visualization of cellular structures, facilitating microscopic analysis. Developing safe, cost-effective, and environmentally friendly natural dyes is essential for sustainable histological applications. Tannin dye extracted from *C. tagal* binds effectively to cotton cellulose, indicating its potential for plant tissue staining. This study evaluates the visibility of stained plant tissues, mordant selectivity, color contrast optimisation, and chemical bonding interactions. The stem sections of sunflower (*Helianthus annuus* L.) were stained with *C. tagal* tannin dye. Mordants used included ferrous sulfate ($FeSO_4$), aluminum sulfate ($Al_2(SO_4)_3$), and calcium carbonate ($CaCO_3$), with synthetic safranin serving as a control. Color contrast optimization was performed using response surface methodology (RSM), analyzing dye concentration, immersion duration, and mordant concentration. Color contrast (ΔE) was measured using colorimetry via a smartphone application, while chemical interactions were examined through Fourier transform infrared (FTIR) spectroscopy. The results showed that tannin dye adhered well to plant tissues, producing colors ranging from sepia brown to baker's chocolate. $Al_2(SO_4)_3$ produced the highest contrast ($\Delta E = 79.7$). Optimal staining conditions were achieved with 44.233 g/L tannin dye, 73.636 s of immersion, and 110.454 g/L $Al_2(SO_4)_3$ as the mordant. FTIR analysis revealed bonding interactions, evidenced by peak intensity shifts at 2922 and 1100 cm^{-1}. *C. tagal* tannin dye demonstrates strong potential as a natural, sustainable plant tissue stain with effective mordant selectivity and contrast. Further research is recommended to expand its application across diverse plant species and to standardize protocols for broader histological use.

Keywords: *Ceriops tagal*, color contrast, natural dye, selectivity, tannin, tissue staining, visibility

1. INTRODUCTION

The study of biology at the cellular and tissue levels fundamentally relies on laboratory-based activities involving microscopic analysis. Laboratory practices are essential in enhancing students' understanding of biological concepts by providing opportunities for direct observation of cellular structures, rather than relying solely on theoretical explanations [1][2]. However, microscopic examination of cells and tissues poses significant challenges due to the transparent nature of specific cellular components, which limits their ability to absorb or refract light effectively. This limitation is caused by the low pigment content or the complete absence of pigments in some cells, making it difficult to distinguish specific structures under a microscope [3]. Consequently, applying staining and fixation techniques becomes essential for improving the visualization of cellular and tissue structures, thereby enabling more precise observation and analysis [4][5].

Tissue staining is a crucial technique for enhancing contrast and improving the visualization of cellular components, thereby facilitating their observation, differentiation, and analysis [6]. However, cellular organelles do not interact uniformly with staining agents due to differences in their structural composition and chemical properties [7][8]. Each organelle has distinct physicochemical characteristics, resulting in varying affinities for specific stains. Prior to staining, tissue samples must undergo a series of preparatory steps to optimize contrast and ensure that cellular structures are clearly distinguishable under microscopic examination [9]. During staining, the dye interacts with particular tissue components. Once bound, the dye absorbs light at specific wavelengths, making the tissue visibly colored and enhancing the

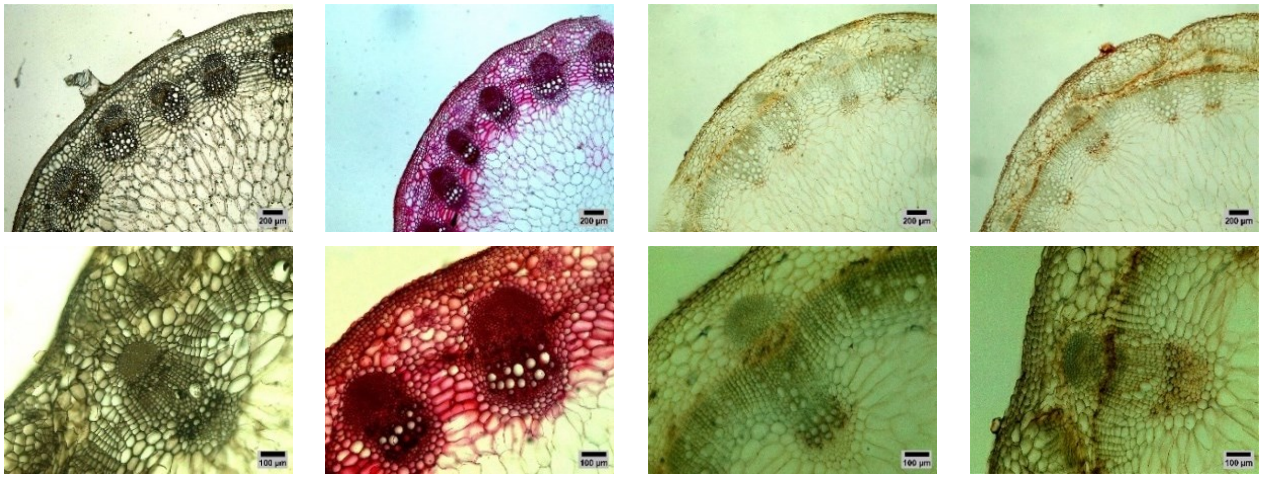

(a) (b) (c) (d)

Figure 1. Cross-section of sunflower (*H. annuus*) stem tissue: (a) unstained stem tissue, (b) stem tissue stained with safranin at a concentration of 10 g/L for 60 min, (c) stem tissue stained with tannin at a concentration of 30 g/L for 60 min, and (d) stem tissue stained with tannin at a concentration of 60 g/L for 60 min. The upper row shows images captured at 40× magnification, while the lower row presents the corresponding tissues observed at 100× magnification.

distinction between different structures [10]-[12].

Synthetic dyes are widely used in tissue staining, including safranin [13], eosin [14], methylene blue [15][16], and brilliant blue [17]. However, their use raises several health and environmental concerns, such as toxicity, carcinogenicity [18], and allergic reactions [17]. As a result, natural dyes are increasingly promoted as safer alternatives to mitigate these risks [17][19]. In addition to their lower toxicity and improved biocompatibility [20], natural dyes offer environmental sustainability due to their biodegradability [21]. Despite abundant local natural resources, their potential as biological learning tools remains underutilized. Therefore, integrating ethnobiology-based approaches into biology practicums is essential for preserving local cultural knowledge, including using plants as natural dyes [22][23]. Numerous plant species in the surrounding environment have the potential to serve as alternative sources of natural dyes [24][25]. These dye pigments can be extracted from various plant parts, including stems, leaves, flowers, fruits, and roots [26].

Several natural pigments have been investigated for their staining properties, including yellow pigments from turmeric (*Curcuma longa* Linn) [27], anthocyanins from pomegranate (*Punica granatum* L) [28], betalains from beetroot (*Beta vulgaris* L) [29], and carotenoids from carrots (*Daucus carota* L) [30][31]. Additionally, red pigments can be derived from anthocyanins present in dragon fruit (*Hylocereus costaricensis*) peel extract [32]. Tannins, another class of natural dyes, are abundant in tea, coffee, and grapes [33], as well as in various plant species such as *Berberis thunbergii* [34], *Hibiscus sabdariffa* [35], *Biancaea sappan* [36], and sweet orange (*Citrus sinensis*) peel [37]. Furthermore, tannins can be extracted from the bark of the mangrove tree *C. tagal*, which produces a reddish-brown pigment [38].

Tannin is a polyphenolic compound soluble in water and alcohol due to its hydroxyl and phenolic functional groups, facilitating interactions with metal ions [20][39]. Beyond its role as a natural dye, tannin also functions as a mordant by forming stronger and more wash-resistant bonds when complex with metal ions [40]. Combining tannin with mordants enhances color stability and reduces fading [41]. Mordants are generally classified into metallic salts, oil-based mordants, and tannin-based mordants [42]. In fabric dyeing, tannin effectively binds to cellulose fibers in cotton textiles [43][44]. The absorbed tannin forms ionic bonds with hydroxyl groups in cellulose, ensuring strong color retention even after repeated washing with water and detergent [45]. Tannin extracted from *C. tagal*

bark has been shown to bind efficiently with cellulose fibers in cotton fabrics [46]. Consequently, tannin-based dyes hold significant potential as environmentally friendly tissue-staining agents [41] and offer additional health benefits [47].

Tannin-based dyes have not yet been extensively explored for *in vivo* tissue staining. Plant tissues comprise various macromolecules, including carbohydrates, proteins, lipids, nucleic acids, and minerals. The plant cell wall comprises carbohydrate polymers such as cellulose, hemicellulose, and lignin [48]. Additionally, plants contain distinct tissue types, including the epidermis, sclerenchyma, collenchyma, xylem, and phloem, each exhibiting unique structural characteristics and specialized functions [49]. Tannin-based dyes, derived from plant polyphenols, offer promising eco-friendly solutions due to their natural origin, biodegradability, and affinity for biological tissues. *C. tagal*, a mangrove species rich in hydrolyzable and condensed tannins, presents potential as a source of natural dye for histological purposes. Previous studies have noted the strong binding affinity of tannins to cellulose-rich substrates such as cotton, indicating potential effectiveness in staining plant tissues.

This study aims to evaluate the staining performance of tannin dye extracted from *C. tagal* bark on plant tissues, focusing on four key aspects: visibility of tissue structures, selectivity of mordant interaction, optimization of staining parameters, and the nature of dye–tissue chemical interactions. The research specifically utilizes transverse sections of sunflower (*H. annuus*) stems to assess the applicability of this natural dye in plant histology. Three mordants—ferrous sulfate ($FeSO_4$), aluminum sulfate ($Al_2(SO_4)_3$), and calcium carbonate ($CaCO_3$)—were tested to evaluate their influence on color contrast and dye binding. The main hypotheses of this study are as follows *C.*

Table 1. Color contrast between stained and unstained sunflower stem tissues, measured under different staining conditions for 60 minutes.

	Stained			Unstained			ΔE
	L*	a*	b*	L*	a*	b*	
Tissue stained with 10 g/L safranin	10.2	30.5	40.8	0	1.9	7.5	**111**
Tissue stained with 30 g/L tannin dye	42.4	12.8	49.6	0	1.9	7.5	**148.9**
Tissue stained with 60 g/L tannin dye	19.2	22.1	55.5	0	1.9	7.5	**127**

Note: L*= lightness; a*= red/green value; b*= blue/yellow value; ΔE= color contrast

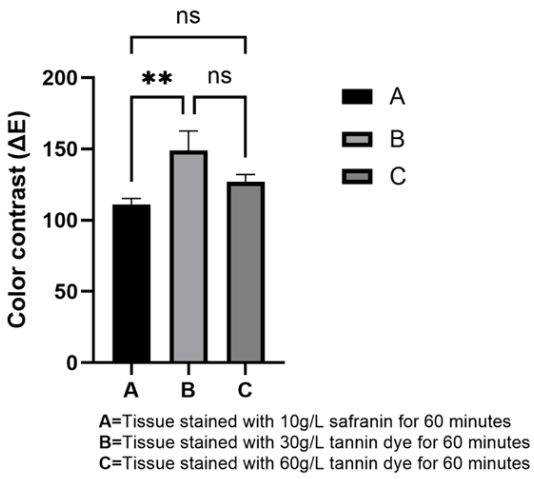

Figure 2. Mean color contrast (ΔE) of plant tissues after 60 minutes of staining under three different treatments: A = 10 g/L safranin, B = 30 g/L tannin from *C. tagal*, and C = 60 g/L tannin from *C. tagal*. The color contrast values were calculated based on differences in staining intensity. ** indicate statistically significant differences ($p < 0.01$), while "ns" denotes non-significant differences ($p > 0.05$).

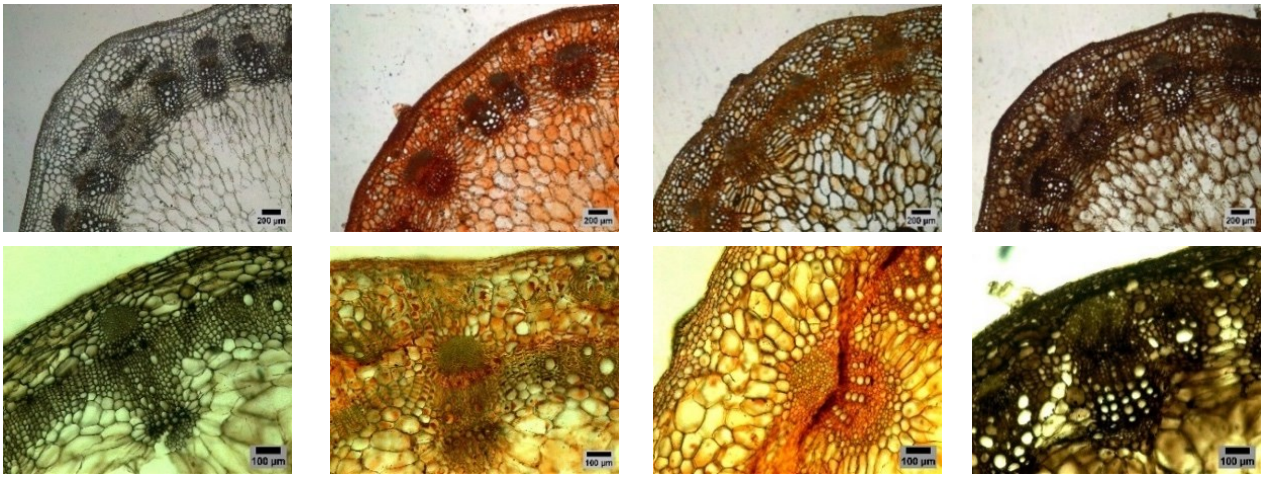

(a) **(b)** **(c)** **(d)**

Figure 3. Cross-section of sunflower stem tissue stained with a natural tannin dye at a concentration of 60 g/L, with an immersion time of 60 s, under different mordant treatments (60 g/L): (a) unstained control, (b) $CaCO_3$, (c) $Al_2(SO_4)_3$, and (d) $FeSO_4$. The upper row shows images captured at 40× magnification, while the lower row presents the corresponding tissues observed at 100× magnification.

tagal tannin dye can effectively stain plant tissue with distinct visibility and contrast, different mordants significantly influence dye–tissue interaction and color output, and optimal staining conditions can be statistically determined through response surface methodology (RSM). By investigating these hypotheses, this study contributes to the development of sustainable, cost-effective, and environmentally safe alternatives to synthetic dyes in plant histology.

2. MATERIALS AND METHODS

2.1. Materials

The natural dye used in this study was liquid tannin, extracted from the bark of *C. tagal*. The tannin dye was produced by Gama Indigo Yogyakarta [46]. The liquid dye was evaporated at room temperature in an open container to increase its concentration. The final tannin concentration was determined using the gravimetric method [50]. Safranin was used as a control stain. The plant tissue sample used in this study was the stem of a two-month-old sunflower (*H. annuus*) plant. The stem was collected from a 10 cm section above the root base. It was then cleaned, rinsed with distilled water, and cut into 2 cm sections. These sections were transversely sliced using a sliding microtome to obtain thin sections with a 20–30 µm thickness. The tissue sections were subsequently placed in a Petri dish containing 70% ethanol for preservation.

2.2. Methods

2.2.1. Plant Tissue Visibility Test

To evaluate its staining properties, the tannin-based natural dye extracted from the bark of Ceriops tagal was applied to transverse sections of sunflower stem tissues. The samples were divided into four treatment groups: (1) unstained tissue as the negative control, (2) tissue stained with 1% safranin for 60 min as the positive control, (3) tissue stained with 3% (30 g/L) tannin dye for 60 min, and (4) tissue stained with 6% (60 g/L) tannin dye for 60 min. These treatments were designed to compare the staining effectiveness of tannin dye at different concentrations and exposure times with that of the conventional safranin stain.

The plant tissue sections were immersed in their respective dye solutions according to the designated treatment conditions, with immersion times precisely measured using a stopwatch. Following staining, the sections were blotted dry with filter paper and subjected to a graded ethanol dehydration series (30%, 50%, 70%, 80%, 90%, and 100%) to remove excess water and enhance sample preservation. The dehydrated sections were treated

sequentially with alcohol–xylene mixtures in volume ratios of 3:1, 1:1, and 1:3, followed by immersion in pure xylene I and II for 60 s each. Before the samples dried completely, Canada balsam was applied as a mounting medium, and a coverslip was immediately placed over the samples to ensure proper adhesion and long-term preservation [51]. The prepared slides were labeled and left to dry until the Canada balsam fully solidified. The stained tissue sections were subsequently examined under a light microscope, and images were captured using a Leica optical microscope for further analysis.

2.2.2. Selectivity Test of Tannin Dye with Mordants

Sunflower stem tissues were stained using a tannin-based natural dye extracted from *C. tagal* bark and treated with different mordants under standardized conditions. The staining process was conducted using a tannin concentration of 40 g/L, an immersion time of 60 s, and a mordant concentration of 60 g/L. The experimental groups consisted of four treatments: (1) unstained tissue as the negative control, (2) tissue stained with tannin dye combined with $CaCO_3$ as a mordant, (3) tissue stained with tannin dye and $Al_2(SO_4)_3$ as a mordant, and (4) tissue stained with tannin dye and $FeSO_4$ as a mordant. These treatments were designed to assess the impact of different mordants on stain adherence, tissue contrast, and color stability.

The tissue sections were immersed in dye solutions of varying concentrations, with immersion times precisely monitored using a stopwatch. After staining, the samples were gently blotted dry with filter paper and subsequently immersed in the designated mordant solutions according to the experimental conditions. The sections were then dehydrated through a graded ethanol series (30%, 50%, 70%, 80%, 90%, and 100%), followed by sequential treatment with alcohol-xylene mixtures at volume ratios of 3:1, 1:1, and 1:3, and finally immersed in pure xylene I and II for 60 s each. Before complete drying, Canada balsam was applied, and coverslips were carefully placed over the sections to preserve the stained tissues. The prepared slides were labeled and left to dry until the Canada balsam fully solidified. The stained tissue samples were subsequently examined under a light microscope and documented through photomicrography.

2.2.3. Optimization of Staining in Plant Tissue Preparations

The study employed RSM using a central composite design (CCD) approach to optimize the staining process. The experimental factors included tannin dye concentration (20, 40, and 60 g/L) [46], immersion time (20, 40, and 60 s), and Al^{3+} mordant concentration (30, 60, and 90 g/L). RSM utilizes mathematical and statistical modeling to

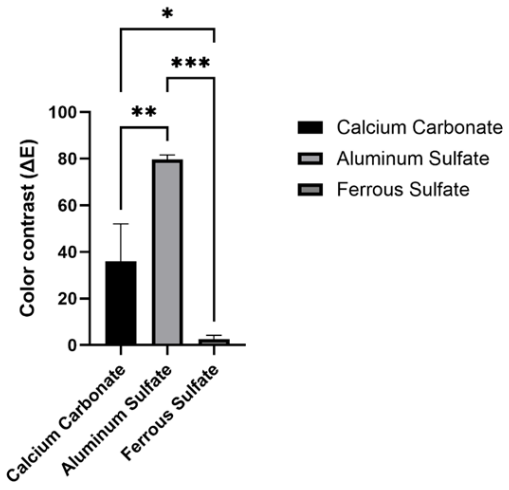

Figure 4. Color contrast (ΔE) of tissues after staining with tannin from *C. tagal* combined with three types of mordants: $CaCO_3$, $Al_2(SO_4)_3$, and $FeSO_4$. The highest ΔE value was obtained with the use of $Al_2(SO_4)_3$. The asterisk * indicates a significant difference ($p < 0.05$), ** indicates a highly significant difference ($p < 0.01$), and *** indicates a very highly significant difference ($p < 0.001$).

Table 2. Color contrast of sunflower stem tissue stained with tannin dye using different mordants.

	Unstained			$CaCO_3$			$Al_2(SO_4)_3$			$FeSO_4$		
	L*	a*	b*	L*	a*	b*	ΔE	L*	a*	b*	ΔE	
The darkest stained tissue	13.6	2.0	4.5	11.3	26.9	46.3	64.5	21.2	29.6	58.7	89.5	0	2	1.1	17
The lightest stained tissue	80.8	-2.7	6.,8	88.9	4.1	20.4	28.5	90.4	-4.8	9.1	9.7	95	-2.2	8.3	16.1
Color Contrast	67.2	-4.7	2.3	77.6	22.8	25.9	**35.9**	69.2	34.4	49.7	**79.7**	95	-4.3	7.2	**0.9**

analyze the relationships between multiple independent variables (X) and a response variable (Y), enabling the determination of optimal conditions [52]. A key advantage of RSM is its ability to account for interaction effects among variables, thereby minimizing the number of experimental trials required to evaluate multiple parameters and their interactions. This approach enhances experimental efficiency by reducing time and costs [53]. The staining procedure for tissue optimization followed the same protocol as the tissue visibility test.

2.2.4. Analysis of Interactions Between Plant Tissue, Tannin-Based Natural Dye, and Al^{3+} Mordant

The optimal staining conditions identified through the RSM response analysis were further evaluated to examine functional group interactions in different treatment groups: (a) unstained plant tissue, (b) plant tissue stained with tannin-based natural dye, and (c) plant tissue stained with tannin-based natural dye combined with an Al^{3+} mordant. Fourier transform infrared (FTIR) analysis was performed using a Thermo Scientific Nicolet iS10 FTIR spectrometer. The study was conducted over a wavelength range of 4000–400 cm^{-1} to detect molecular bond vibrations and identify functional groups. FTIR spectroscopy measures infrared absorption by chemical bonds, generating spectra that provide insights into molecular interactions between the dye, mordant, and plant tissue components. The results were presented in percentage transmittance and wavenumber, enabling a detailed interpretation of functional group presence and bonding characteristics [54] [55].

2.2.5. Data Collection and Analysis

Microscopic observations of stained tissue preparations were performed using an optical microscope, with images captured using a Leica optical microscope. The specimens were observed under a microscope at 40×, 100×, and 400x magnifications and subsequently photographed using a Leica ECC 5 optical microscope at a resolution of 1600×1200 pixels, with a color bit depth of 24 bits per pixel. Exposure settings were uniformly adjusted for all specimens. The photos

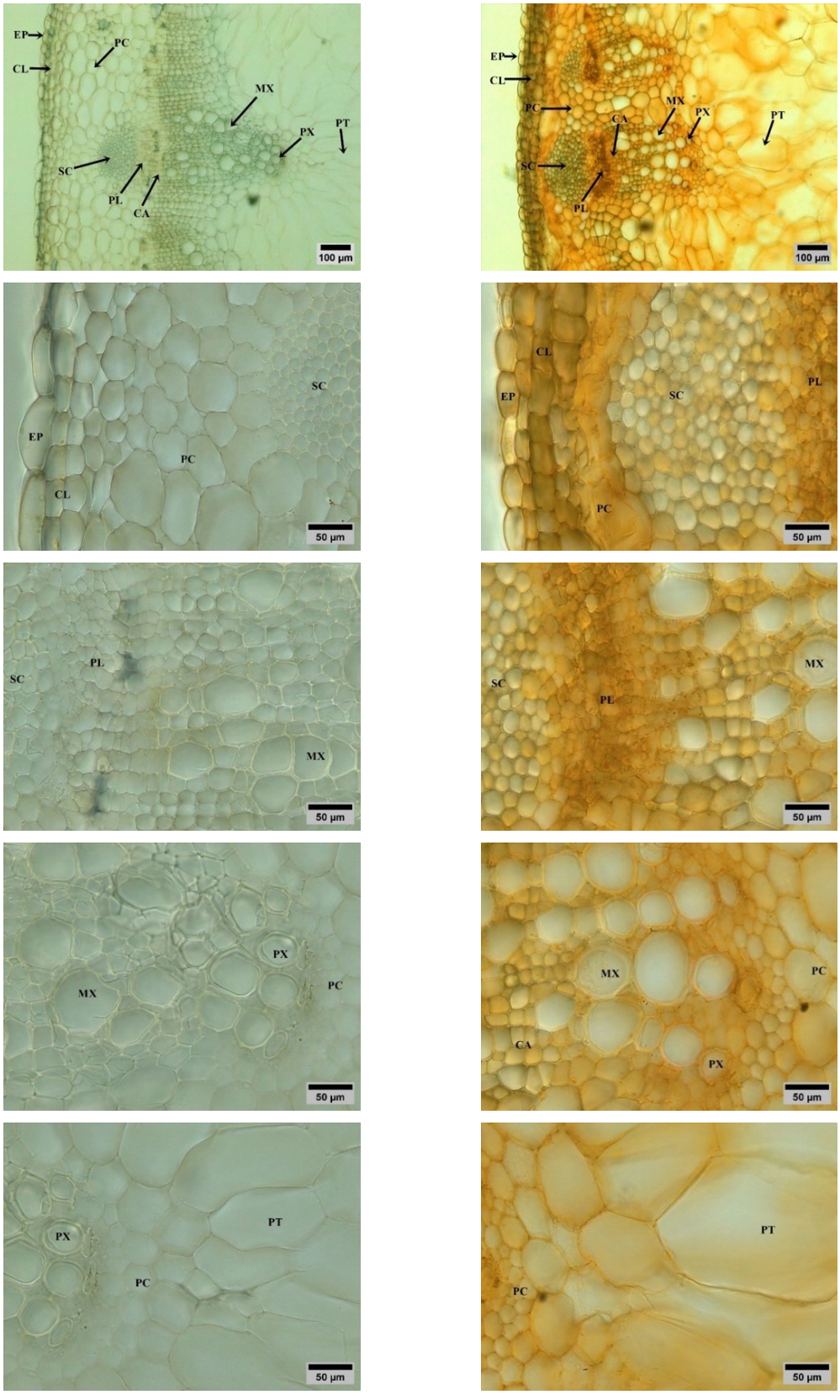

Figure 5. Cross-section of sunflower stem tissue with different staining treatments: (a) unstained, (b) stained with natural tannin dye extracted from *C. tagal* at a concentration of 60 g/L, with an immersion time of 60 s and $Al_2(SO_4)_3$ as a mordant. The top images were captured at 100× magnification, while the bottom images show the same tissues observed at 400× magnification.

Note: EP: epidermis, CL: collenchyma, PC: parenchyma, SC: sclerenchyma, PL: phloem, CA: cambium, MX: metaxylem, PX: protoxylem, PT: pith.

are saved in jpg format. The photos are transferred to a smartphone to be analyzed for color with a colorimeter application to determine Lab* values, which quantify color characteristics based on the CIE Lab color scale. L* represents lightness in this scale, ranging from 0 (black) to 100 (white). The a* value indicates the red-green axis, where negative values (-a*) correspond to green and positive values (+a*) correspond to red, ranging from -128 to +127. Similarly, the b* value represents the blue-yellow axis, with negative values (-b*) indicating blue and positive values (+b*) indicating yellow, also within a range of -128 to +127. The ΔE equation (Eq. 1) was applied to evaluate color contrast between samples, providing a quantitative measure of color variation;

$$\Delta E = [(L*'-L*)2 + (a*'-a*)2 + (b*'-b*)2]1/2 \quad (1)$$

where L*', a*', and b*' represent the color values of the treated samples, while L*, a*, and b* correspond to the color values of the control samples [56]-[58].

The ΔE values were used to assess the optimal color contrast in stained plant tissue preparations. Data analysis was conducted using RSM with Design Expert version 13 software [59]. The color contrast between unstained (control) and stained tissues indicated tissue visibility, suggesting that the dye successfully adhered to the tissue, resulting in visible coloration. The contrast was determined by comparing the most intensely stained regions with the least stained areas and calculating the color contrast (ΔE).

3. RESULTS AND DISCUSSIONS

3.1. Plant Tissue Visibility

In this study, tannins function as natural dyes extracted from the bark of *C. tagal*, obtained in liquid form with a reddish-brown hue. These natural dyes have been successfully applied in batik fabric dyeing [46], and they also exhibit promising potential in plant tissue staining. As shown in Figure 1, the tannin extract effectively stained the stem tissues of sunflower. A concentration of 60 g/L applied for 60 min produced the darkest shade, identified as wine red, while a 30 g/L concentration with the same immersion time resulted in a saddle brown color. In contrast, the unstained sunflower stem tissues appeared gray, making structural details less discernible compared to those stained with tannins. For comparison, synthetic dyes such as safranin are among the most commonly used stains in plant tissue histology. In this study, staining with 60 g/L tannin for 60 min also yielded a Barossa violet shade. The range of colors produced by tannins highlights their potential as alternative staining agents for plant tissues. Tannin, or tannic acid, can appear colorless, yellow, or light brown, and upon exposure to sunlight, it undergoes hydrolysis resulting in a darker brown color. Additionally, tannins can react with metal ions to form blue-black pigments [60], although they

Table 3. Color contrast between tissues in sunflower stem stained with natural tannin dye extracted from *C. tagal* bark at a concentration of 60 g/L, with an immersion time of 60 s, using $Al_2(SO_4)_3$ as a mordant.

No.	Tissue	L*	a*	b*	ΔE
1	Collenchyma	65.6	8.8	59.6	109.0
2	Parenchyma	62.9	9.8	60.5	91.2
3	Epidermis	71.7	4.3	50.0	83.8
4	Pith	58.1	8.7	52.4	65.9
5	Protoxylem	63.1	4.3	42.5	59.6
6	Phloem	50.3	13.3	51.9	57.9
7	Metaxylem	74.1	-2.9	40.2	56.5
8	Cambium	53.8	1.3	40.5	27.7
9	Sclerenchyma	65.6	-5.0	35.8	12.6

Note: L*= lightness; a*= red/green value; b*= blue/yellow value; ΔE= color contrast

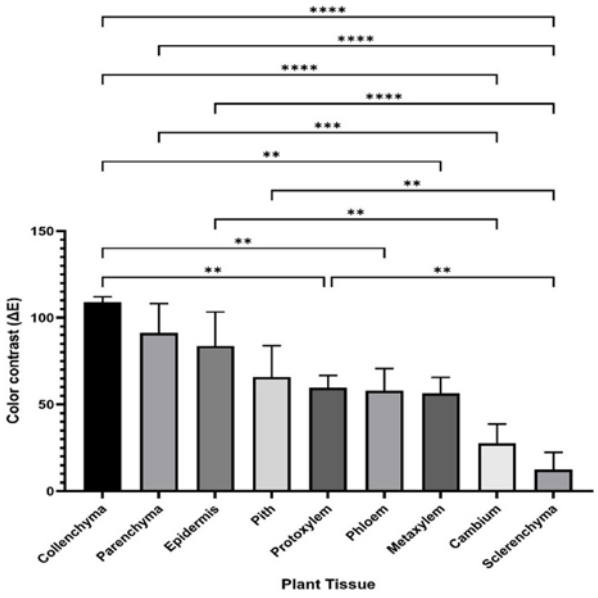

Figure 6. Comparison of ΔE in various plant tissues. The graph shows the average color contrast values for each type of tissue. Collenchyma tissue exhibits the highest color contrast, while sclerenchyma has the lowest. Asterisks indicate the level of statistical significance of the differences between tissue pairs: **p < 0.01; ***p < 0.001; ****p < 0.0001.

generally produce dull brown tones [61].

Figure 1 illustrates the differences in staining outcomes of sunflower stem tissue using tannin and safranin. Staining with tannin (30 and 60 g/L) for 60 min resulted in uneven coloration, predominantly concentrated in the epidermis, parenchyma, and phloem, while other tissue regions exhibited weaker staining. In contrast, safranin staining demonstrated a more uniform distribution across all stem tissues. The inconsistent tannin binding may be attributed to pigment leaching during the sequential washing process with water and graded alcohol. This phenomenon is comparable to tannin-based dyeing of cotton fabric, where a mordant is required to enhance tannin fixation within cellulose fibers [40].

Based on Table 1, the color contrast (ΔE) count on plant tissues stained using safranin and tannin extracted from *C. tagal*, a variable contrast contrast was observed across treatments. Tissues stained with 10 g/L safranin for 60 minutes immersion exhibited the lowest color contrast compared to the other two treatments involving tannin. Figure 2, tissue staining with 30 g/L tannin for 60 minutes showed a significantly higher color contrast compared to safranin, as indicated by the symbol ** on the graph. This symbol denotes that the difference between A and B tannin staining at concentrations of 30 (60-min immersion) anda safranin staining at concentrations of 10 (60-min immersion) was statistically significant ($p < 0.01$). This result suggests that tannin from *C. tagal* is capable of providing a stronger or more pronounced staining effect compared to the synthetic dye safranin at the tested concentration. However, no significant difference in color contrast was observed between tannin staining at concentrations of 30 and 60 g/L (60-min immersion), as indicated by the "ns" (not significant) label on the graph. A similar pattern was observed when comparing tissues stained with 10 g/L safranin and 60 g/L tannin a for 60 min immersion. Although there was a trend of increased contrast from tissues stained with 10 g/L safranin to 60 g/L tannin a for 60 min immersion, the increase was not statistically significant.

This lack of significance indicates that increasing the tannin concentration from 30 g/L to 60 g/L does not result in a substantial improvement in color contrast. Therefore, the use of tannin at a concentration of 30 g/L is already effective in achieving maximum staining intensity under the same duration (60 min). These findings suggest that tannin extracted from *C. tagal* has the potential to serve as a natural alternative to synthetic dyes such as safranin, with comparable or even superior efficacy in enhancing tissue color contrast.

Table 4. Color contrast in sunflower stem tissues stained with natural tannin dye from *C. tagal* bark and fixed with $Al_2(SO_4)_3$ using RSM.

Run	Factor 1	Factor 2	Factor 3	Response			
	Tannin Dye	Mordant	Immersion Time				
	g/L	g/L	Second	L*	a*	b*	ΔE
1	40	60	40	54.9	35.1	75.7	115.0
2	73.6	60	40	6.6	9.5	20.2	14.4
3	20	30	60	55.7	22.7	32.8	60.5
4	60	90	20	54.7	31.6	64.1	99.7
5	60	30	60	57.1	31.2	55.6	93.2
6	40	110.45	40	57.0	25,4	60.3	92.0
7	60	30	20	65.2	30.2	55.6	100.3
8	40	60	6.4	50.2	25.9	63.3	88.7
9	40	10	40	47.2	29.7	68.3	94.5
10	40	60	40	47.3	26.4	66.0	89.0
11	6.4	60	40	31.3	3.3	30.4	14.3
12	60	90	60	52.3	28.8	68.6	99.0
13	20	90	20	51.2	16.3	30.1	46.9
14	20	30	20	42.5	25.5	41.7	59.0
15	40	60	40	49.3	28,1	65.7	92.4
16	20	90	60	38.2	23.9	47.1	58.5
17	40	60	40	56.0	36.6	70.8	112.7
18	40	60	74	74.2	22.3	54.8	100.6
19	40	60	40	53.7	33.6	68.4	105.0
20	40	60	40	48.8	27.6	68.3	94.0

Note: L*= lightness; a*= red/green value; b*= blue/yellow value; ΔE= color contrast

Furthermore, efficiency can be optimized by using the lower concentration of tannin (30 g/L), as increasing the dosage to 60 g/L offers no additional significant benefit. These findings demonstrate that tannin extracted from *C. tagal* bark can stain sunflower stem tissues, albeit with selective affinity. In contrast, safranin, a widely used histological stain, binds effectively to lignin and cellulose, enabling more uniform staining across plant tissues [62].

Tannin staining successfully imparted coloration to sunflower stem tissues; however, it required a longer immersion time and exhibited uneven staining due to pigment leaching during the washing process. This highlights the need for further optimization to establish ideal staining conditions that enhance color contrast and uniformity while reducing processing time. Tannin-cellulose interactions are known to be stronger under acidic conditions, as tannic acid functions as a natural mordant in textile dyeing by forming hydrogen bonds with cellulose through hydroxyl groups. Maximum tannin absorption in cellulose typically occurs after over two hours [63]. Additionally, applying metal-based mordants, either pre-mordants or post-mordants, enhances tannin fixation within cellulose fibers, thereby reducing color leaching and improving dye retention during washing [64].

3.2. Selectivity of Tannin Dye with Mordants

The selectivity of sunflower tissue staining was analyzed using a natural tannin dye extracted from *C. tagal* bark, with a tannin concentration of 60 g/L,

an immersion time of 60 s, and variations in mordants. The mordants used in this study included $CaCO_3$, $Al_2(SO_4)_3$, and $FeSO_4$, each at a concentration of 60 g/L. The resulting tissue coloration is presented in Figure 3, while the quantification of color contrasts, measured using a digital smartphone colorimetry application, is shown in Table 3.

Figure 3 illustrates the dominant color variations observed in tissues stained with different mordants: wine red with $CaCO_3$, black with $FeSO_4$, and red oxide with $Al_2(SO_4)_3$. In Figures 3(b) and 3(d), the entire tissue structure, including the epidermis, parenchyma, vascular bundles, and stele, is thoroughly stained due to strong fixation. In contrast, Figure 3(c) shows dye accumulation predominantly in the vascular tissue, particularly in the phloem. Using $CaCO_3$ and $FeSO_4$ resulted in excessive dye aggregation, which persisted despite washing with water and alcohol. Meanwhile, $Al_2(SO_4)_3$ facilitated a more uniform stain absorption. Adding mordants enhanced color retention and intensified the staining effect, producing more distinct and durable coloration [65]. Similarly, tannin dyes extracted from *C. tagal* bark, when applied to cotton fabric, made a light brown shade with $Al_2(SO_4)_3$ as a mordant, a dark brown shade with $CaCO_3$, and a black hue with $FeSO_4$ [46]. Furthermore, tannin-based dyes derived from *Peltophorum pterocarpum* bark, coffee (*Coffea arabica*) leaves, and guava leaves exhibited color variations ranging from cream to reddish-brown when treated with $Al_2(SO_4)_3$ as a mordant [66]. These findings highlight the crucial role of mordants in modifying dye-binding properties, thereby influencing stain intensity, color stability, and potential applications in histological staining and textile dyeing.

The results in Table 2 show that the highest ΔE in sunflower stem tissue stained with natural tannin dye extracted from *C. tagal* was observed when $Al_2(SO_4)_3$ was used as a mordant, with a ΔE value of 79.7. Conversely, the lowest color contrast was recorded with $FeSO_4$, yielding an ΔE value of 0.9. Figure 4 indicates that the asterisks denote statistically significant differences among all comparisons of the three mordant types in producing color contrast in the stained tissues. $Al_2(SO_4)_3$ was the most effective mordant, yielding the highest color contrast values, while $FeSO_4$ was the least effective. The application of $Al_2(SO_4)_3$ significantly enhanced the staining performance of *C. tagal* tannin. Conversely, $FeSO_4$ appeared to be unsuitable for use with *C. tagal* tannin, as it resulted in markedly low staining intensity. The application of mordants significantly reduced the immersion

Table 5. Statistical analysis of ANOVA for the response surface quadratic model.

Source	Sum of Squares	df	Mean Square	F-value	p-value	
Model	13961.74	9	1551.30	6.12	0.0045	significant
A-Tannin	2053.59	1	2053.59	8.11	0.0173	
B-Mordant	12.57	1	12.57	0.0496	0.8282	
C-time soaking	46.92	1	46.92	0.1852	0.6760	
AB	46.56	1	46.56	0.1838	0.6772	
AC	54.60	1	54.60	0.2156	0.6524	
BC	34.03	1	34.03	0.1344	0.7216	
A^2	11520.21	1	11520.21	45.48	< 0.0001	
B^2	2.06	1	2.06	0.0081	0.9299	
C^2	0.1969	1	0.1969	0.0008	0.9783	
Residual	2532.88	10	253.29			
Lack of Fit	1917.77	5	383.55	3.12	0.1188	not significant
Pure Error	615.12	5	123.02			
Cor Total	16494.63	19				

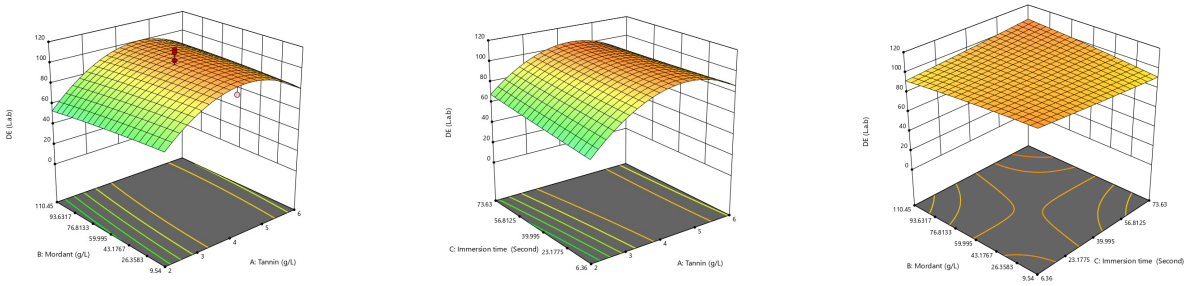

(a) **(b)** **(c)**

Figure 7. 3D surface plots of ΔE as a function of (a) tannin dye concentration and mordant concentration, (b) tannin dye concentration and immersion time, and (c) mordant concentration and immersion time.

time required for tannin dye absorption, as they facilitated rapid binding and retention of the dye within the tissue. Mordants function as complex-forming agents that improve dye fixation and enhance color uptake. This process substantially influences color properties and fastness, with each dye-mordant interaction yielding distinct staining results depending on the type and application method of the mordant [67].

The study further demonstrated that $Al_2(SO_4)_3$ resulted in the brightest coloration, whereas $FeSO_4$ produced the darkest stain. These findings align with reports that aluminum-based mordants generate the highest L* values, while iron-based mordants produce the lowest L* values and the darkest coloration [68]. Metal-polyphenol complexes formed with aluminum mordants generally produce clear yellow hues, whereas samples treated without mordants or solely with tannins tend to appear light brown [40]. When dissolved in water, $Al_2(SO_4)_3$ dissociates into aluminum ions (Al^{3+}) and sulfate ions (SO_4^{2-}), which lowers the pH and creates an acidic environment conducive to dye binding [69]. Tannic acid has a strong affinity for Al^{3+} due to the presence of catechol and galloyl groups in its molecular structure, which serves as preferential binding sites for aluminum ions, forming stable dye -metal complexes [70]. Additionally, the carboxyl groups in polysaccharides and the hydroxyl and oxyl groups in tannin compounds play a crucial role in metal conjugation and dye fixation [71].

Based on Figure 5, the comparison between tissues stained with tannin using $Al_2(SO_4)_3$ as a mordant and unstained control tissues reveals that the dye binds to all tissue types, albeit with varying intensities. The most pronounced staining is observed in the phloem tissue, which exhibits a gold-orange hue, while the phloem fibers (sclerenchyma) display lower dye absorption. Additionally, parenchyma tissue appears darker than xylem fibers, likely due to lignin and cellulose content differences. When used with mordants, tannin dyes interact more effectively with cellulose-rich materials, enhancing their binding stability [44].

The results of color intensity measurements on the cell walls of sunflower stem tissues using a smartphone colorimetry application are presented in Table 3. Tissues with the highest color contrast include the collenchyma, parenchyma, epidermis, and pith, while sclerenchyma exhibits the lowest contrast. The data presented in Figure 6 demonstrate statistically significant differences in ΔE among the various plant tissues analyzed. Higher ΔE values reflect more pronounced visual distinctions between tissues. Statistical analyses reinforce these observations, revealing that the differences in ΔE among several tissue pairs are highly significant ($p < 0.0001$). The elevated ΔE value in collenchyma is likely attributable to its characteristic unevenly thickened cell walls and the presence of cell wall components such as cellulose. These structural features may enhance the binding affinity of natural tannin dyes, thereby producing more intense coloration and higher contrast. Conversely, cambium and sclerenchyma showed the lowest ΔE values. Sclerenchyma, a highly lignified mechanical tissue with heavily thickened secondary cell walls, appears to absorb tannin dye poorly, resulting in relatively uniform coloration and diminished visual contrast.

The samples analyzed in this study were 2-month-old stems of sunflower, which show the characteristics of a young dicotyledonous plant. The stem undergoes secondary growth at this developmental stage, leading to thicker cell walls in vascular bundles, xylem, and phloem fibers, which contain higher lignin concentrations than other tissues [49]. The lignification process in vessel cell walls enhances structural support and resistance to pressure during substance transport [72]. These findings align with the results of this study, where tissues stained with tannin appeared darker and more distinct, as tannin preferentially binds to cellulose-rich structures. In contrast, lignin-rich tissues exhibited a lower affinity for tannin staining, resulting in a less intense coloration.

3.3. Optimization of Staining in Plant Tissue Preparations

The optimization of plant tissue staining utilizing tannin dye was undertaken to identify the optimal formulation by assessing the effects of tannin dye concentration, mordant concentration, and immersion time. The experimental design employed RSM with a CCD, encompassing 20 experimental runs. The independent variables (X factors) included tannin dye concentration, $Al_2(SO_4)_3$ mordant concentration, and immersion time, while the response variable (Y) was the ΔE.

Based on the results presented in Table 4, the highest L* value (74) was observed in the experiment conducted with a tannin dye concentration of 40 g/L, a $Al_2(SO_4)_3$ mordant concentration of 60 g/L, and an immersion time of 40 s, indicating a lighter coloration. In contrast, the darkest coloration, with an L* value of 6.6, was recorded in the experiment using a tannin dye concentration of 73.6 g/L, a $Al_2(SO_4)_3$ mordant concentration of 60 g/L, and an immersion time of 40 s. The ΔE between the stained samples and the unstained control showed that the highest ΔE value (115) was achieved with a tannin dye concentration of 40 g/L, an $Al_2(SO_4)_3$ mordant concentration of 60 g/L, and a 40-s immersion time. Conversely, the lowest color contrast (ΔE = 14.4) was observed in the experiment with a tannin dye concentration of 73.6 g/L.

Based on Table 5, the ANOVA results, the overall model was found to be significant, with a p-value of 0.0045. This indicates that the variables included in the model have an effect on the observed response. Among the three main factors tested (tannin, mordant, and soaking time), only the tannin factor (A) had a significant effect on the response, with a p-value of 0.0173. Additionally, the quadratic effect of tannin (A^2) showed a highly significant influence ($p < 0.0001$), indicating a nonlinear relationship between tannin concentration and the response. In contrast, the mordant (B), soaking time (C), their interactions (AB, AC, BC), and the quadratic effects of B and C (B^2 and C^2) did not exhibit significant effects ($p > 0.05$). The Lack of Fit test yielded a p-value of 0.1188, indicating that the model does not suffer from significant lack of fit, and thus provides a reasonably good representation of the data. A response is considered statistically significant when the p-value is less than 0.05. The lack-of-fit test was insignificant ($p = 0.1100$), suggesting that the model accurately represents the data and is well-suited for prediction. The adjusted R^2 value of 0.7082 demonstrates a strong correlation between the independent variables, tannin concentration, mordant concentration, immersion time, and ΔE response. A decline in the adjusted R^2 value typically occurs when additional variables included in the model do not significantly contribute to the reaction [52].

The graphical analysis in Figures 7(a) and 7(b) reveals that ΔE initially increases with increasing tannin concentration. However, further increases in tannin concentration beyond a certain threshold result in a decline in color contrast. Excessive tannin staining causes all tissue structures to be uniformly covered by the dye, leading to a darker overall coloration and reducing the contrast between different tissue components. Conversely,

Table 6. Optimized solutions for plant tissue staining using natural tannin dye extracted from *C. tagal* bark, analyzed using RSM.

Number	Tannin (g/L)	$Al_2(SO_4)_3$ Mordant (g/L)	Immersion time (s)	ΔE	Desirability
1	44.233	110.454	73.636	108.826	0.939

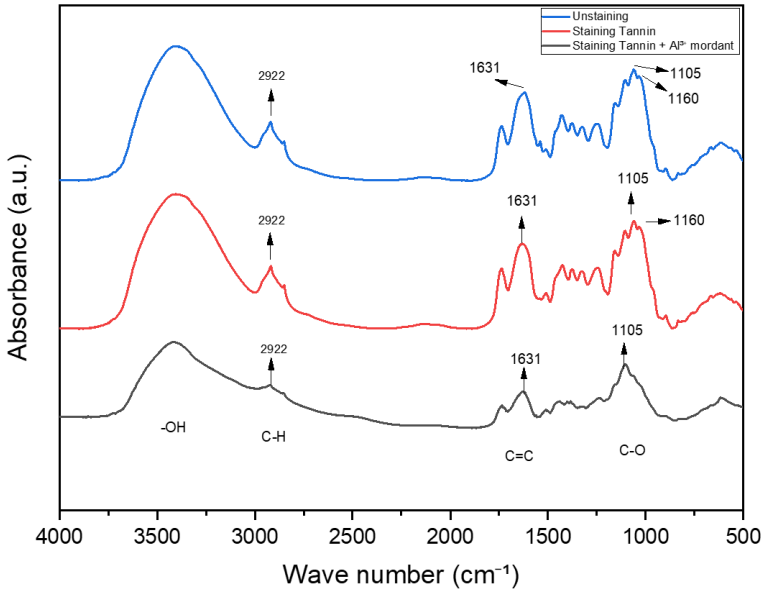

Figure 8. FTIR analysis of chemical bonding interactions between plant tissue, natural tannin dye, and Al^{3+} mordant.

lower tannin concentrations produce lighter staining, reducing ΔE of tissue. In contrast, Figure 7 (c) shows that variations in mordant concentration and immersion time have no significant effect on the ΔE response.

Table 6 presents the results of the RSM analysis, which identifies the optimal conditions for natural tannin dye concentration extracted from *C. tagal* bark, immersion time, and $Al_2(SO_4)_3$ mordant concentration. The optimized parameters determined were a tannin dye concentration of 44.233 g/L, an immersion time of 73.636 s, and a $Al_2(SO_4)_3$ mordant concentration of 110.454 g/L. Under these conditions, the predicted ΔE was 108.826, indicating a high level of staining contrast. Furthermore, the desirability value of the optimized solution was 0.939, suggesting a strong correlation between the model and the experimental data. A desirability value of 1.000 represents an ideal optimization outcome, while a value of 0.000 indicates that the response is unsuitable for use [73].

3.4. Analysis of Chemical Bonding Interactions Between Plant Tissue, Natural Tannin Dye, and Al^{3+} Mordant

The chemical bonding interactions between the stem tissue of *H. annuus* and the natural tannin dye extracted from *C. tagal* bark, using Al^{3+} as a mordant, were analyzed by identifying functional groups through FTIR. Figure 8 presents the absorption peaks within the wavenumber range of 3300–3500 cm^{-1}, corresponding to the stretching vibrations of hydroxyl groups. All samples exhibit relatively similar characteristics at this wavenumber. The absorption peak at 2922 cm^{-1} represents the asymmetric stretching of C–H bonds, while the peak at 1631 cm^{-1} indicates the presence of C=C bonds. Each spectrum, represented by three distinct curves, demonstrates that the absorption peaks of plant tissues stained with natural tannin dye are identical to those of unstained tissues. This suggests that no structural modifications of functional groups occurred between the two samples, and no dipole bonds were formed. However, tannin molecules successfully adhered to plant tissues through hydrogen bonding. The spectra further confirm that plant cell walls primarily consist of carbohydrates, such as cellulose ($(C_6H_{10}O_5)_n$) and lignin, as evidenced by the presence of C=C bonds. Plant cell walls are composed of cellulose microfibrils embedded in a matrix of non-cellulosic polysaccharides and lignin [74].

The observed absorption peaks of cellulose include hydrogen-bonded hydroxylstretching at 3550–3100 cm^{-1}. Infrared absorption bands above 3400 cm^{-1} are associated with intramolecular hydrogen bonding, whereas those below 3400 cm^{-1} correspond to intermolecular hydrogen bonding

[75][76]. The interaction between cellulose and tannin primarily occurs through hydrogen bonding, where the abundant hydroxyl groups in cellulose form hydrogen bonds with hydroxyl and carbonyl groups in tannin [77]. Lignin, the second most abundant component of plant stem tissues, contains various surface functional groups, including phenolic hydroxyl, aliphatic hydroxyl, and methoxy groups, which collectively contribute to its hydrophobic properties. In aqueous-based, eco-friendly dyeing processes, the aromatic components of tannin can interact with the hydrophobic domains of lignin, enhancing the dye's adherence to plant tissues [78].

Figure 8 illustrates distinct differences in absorption peaks between unstained plant tissues and those stained with tannin and $Al_2(SO_4)_3$ mordant. A decrease in peak intensity at 2922 cm^{-1} suggests a reduction in C–H stretching vibrations, indicating potential structural modifications. Conversely, an increase in peak intensity at 1100 cm^{-1} signifies the formation of additional C–O bonds, suggesting a new chemical interaction within the tissue matrix. The chemical bonding between natural tannin dye, $Al_2(SO_4)_3$ mordant, and plant tissues primarily involves ionic interactions with C–O bonds. Due to their polar nature, carbohydrates contain specific binding sites—including hydroxyl and carboxyl groups, that facilitate the adsorption of molecular or ionic species [79]. The electron-rich oxygen atoms in phenolic groups also serve as key binding sites for metal ion adsorption, particularly Al^{3+} ions. Several phenolic compounds in tannin, such as 3-methoxy pyrocatechol, catechol, *p*-vinylphenol, pyrogallol, homovanillic acid, and syringol, play a crucial role in these interactions [70]. These findings further support the hypothesis that tannin-$Al_2(SO_4)_3$ fixation in plant tissues occurs through a combination of ionic and hydrogen bonding, enhancing the stability and effectiveness of the staining process.

4. CONCLUSIONS

To optimize stain contrast in plant tissue preparations, this study investigated the effects of tannin dye concentration, aluminum mordant concentration, and immersion time. The natural tannin dye extracted from *C. tagal* produced strong contrast on sunflower stem tissues, especially with $Al_2(SO_4)_3$, achieving the highest ΔE (79.7) compared to $CaCO_3$ and $FeSO_4$. Non-lignified tissues such as collenchyma, parenchyma, epidermis, and pith showed the most visible staining. Optimal conditions were 44.233 g/L dye, 110.454 g/L Al^{3+}, and 73.636 seconds immersion. FTIR analysis revealed reduced C–H and increased C–O bonding, indicating effective chemical interaction between tannin and tissue components.

AUTHOR INFORMATION

Corresponding Author

Maryani Maryani — Faculty of Biology, Universitas Gadjah Mada,Yogyakarta-55281 (Indonesia);
orcid.org/0000-0002-4871-3224
Email: mmyani@ugm.ac.id

Authors

Rasuane Noor — Doctoral Study Program, Universitas Gadjah Mada,Yogyakarta-55281 (Indonesia); Faculty of Teacher Training and Education, Universitas Muhammadiyah Metro, Metro-34112 (Indonesia);
orcid.org/0000-0003-3034-0092

Bambang Retnoaji — Faculty of Biology, Universitas Gadjah Mada,Yogyakarta-55281 (Indonesia);
orcid.org/0000-0002-0290-9723

Edia Rahayuningsih — Faculty of Engineering, Universitas Gadjah Mada,Yogyakarta-55281 (Indonesia);
orcid.org/0009-0009-5443-9311

Author Contributions

Conceptualization, and Methodology, R. N., M. M., B. R. and E. R.; Software, Investigation, Resources, Data Curation, Visualization, Project Administration, Funding Acquisition, and Writing – Original Draft Preparation, R. N.; Supervision, Validation, Writing – Review & Editing, M. M., B. R. and E. R.; Formal Analysis, R. N. and E. R.

Conflicts of Interest

The authors declare no conflict of interest.

ACKNOWLEDGEMENT

This research supported by Center for Higher Education Funding and Assessment, Ministry of Higher Education, Science, and Technology of Republic Indonesia, BPI (Indonesian Education Scholarship) 2022, under contract number 02104/ J5.2.3./BPI.06/9/2022, and LPDP (Indonesia Endowment Fund for Education).

REFERENCES

[1] A. C. Simatupang and A. F. Sitompul. (2018). "Analisis Sarana Dan Prasarana Laboratorium Biologi Dan Pelaksanaan Kegiatan Praktikum Biologi Dalam Mendukung Pembelajaran Biologi Kelas XI". *Jurnal Pelita Pendidikan.* **6** (2). 10.24114/jpp.v6i2.10148.

[2] D. K. Meyerholz and A. P. Beck. (2018). "Principles and approaches for reproducible scoring of tissue stains in research". *Laboratory Investigation.* **98** (7): 844-855. 10.1038/s41374-018-0057-0.

[3] M. Inyushin, D. Meshalkina, L. Zueva, and A. Zayas-Santiago. (2019). "Tissue Transparency In Vivo". *Molecules.* **24** (13). 10.3390/molecules24132388.

[4] A. L. Mescher. (2024). In: "Junqueira's Basic Histology: Text and Atlas, A. L. Mescher Ed". McGraw Hill. 1-5.

[5] J. G. Cappuccino and N. Sherman. (2018). "Microbiology: A Laboratory manual". Pearson.

[6] P. Dey. (2018). In: "Basic and Advanced Laboratory Techniques in Histopathology and Cytology, ch. Chapter 7". 57-67. 10.1007/978-981-10-8252-8_7.

[7] A. Iswara. (2017). "Pengaruh variasi waktu clearing terhadap kualitas sediaan awetan permanen Ctenocephalides felis". *Jurnal Labora Medika.* **1** (1): 12-15. 10.26714/jlabmed.1.1.2017.12-15.

[8] S. Hassdenteufel and M. Schuldiner. (2022). "Show your true color: Mammalian cell surface staining for tracking cellular identity in multiplexing and beyond". *Current Opinion in Chemical Biology.* **66** : 102102. 10.1016/j.cbpa.2021.102102.

[9] Y. Zhang, K. de Haan, Y. Rivenson, J. Li, A. Delis, and A. Ozcan. (2020). "Digital synthesis of histological stains using micro-structured and multiplexed virtual staining of label-free tissue". *Light: Science & Applications.* **9** : 78. 10.1038/s41377-020-0315-y.

[10] Q. Zhang and W. Liu. (2022). "Transition metal-catalyzed esterification reactions for dye modification: recent developments and future perspectives". *Chemical Reviews Journal.* **98** (7): 1501-1518. 10.6023/cjoc202201006.

[11] A. Kumar, U. Dixit, K. Singh, S. Prakash Gupta, and M. S. Jamal Beg. (2021). In: " Dyes and Pigments - Novel Applications and Waste Treatment, ch. Chapter 8". 10.5772/intechopen.97104.

[12] L. Aztatzi-Rugerio, S. Y. Granados-Balbuena, Y. Zainos-Cuapio, E. Ocaranza-Sanchez, and M. Rojas-Lopez. (2019). "Analysis of the degradation of betanin obtained from beetroot using Fourier transform infrared spectroscopy". *Journal of Food Science and Technology.* **56** (8): 3677-3686. 10.1007/s13197-019-03826-2.

[13] F. Baldacci-Cresp, C. Spriet, L. Twyffels, A. S. Blervacq, G. Neutelings, M. Baucher, and S. Hawkins. (2020). "A rapid and quantitative safranin-based fluorescent microscopy method to evaluate cell wall lignification". *Plant Journal.* **102** (5): 1074-1089. 10.1111/tpj.14675.

[14] S. Koivukoski, U. Khan, P. Ruusuvuori, and L. Latonen. (2023). "Unstained Tissue Imaging and Virtual Hematoxylin and Eosin Staining of Histologic Whole Slide Images". *Laboratory Investigation.* **103** (5): 100070. 10.1016/j.labinv.2023.100070.

[15] E. N. Azka, A. A. Mandasari, and S. D. Santoso. (2021). "Comparison of Natural Dyes from Telang Flower Extracts (Clitoria ternatea L) as a Substitute for Methylen Blue in Diff Quik Painting". *Procedia of Engineering and Life Science.* **1** (2). 10.21070/pels.v1i2.990.

[16] P. O. Oladoye, T. O. Ajiboye, E. O. Omotola, and O. J. Oyewola. (2022). "Methylene blue dye: Toxicity and potential elimination

technology from wastewater". *Results in Engineering.* **16**. 10.1016/j.rineng.2022.100678.

[17] E. O. Alegbe and T. O. Uthman. (2024). "A review of history, properties, classification, applications and challenges of natural and synthetic dyes". *Heliyon.* **10** (13): e33646. 10.1016/j.heliyon.2024.e33646.

[18] V. V. Yurchenko, F. I. Ingel, L. V. Akhaltseva, M. A. Konyashkina, N. A. Yurtseva, T. A. Nikitina, and E. K. Krivtsova. (2021). "Genotoxic safety of synthetic food colours. Review". *Ecological genetics.* **19** (4): 323-341. 10.17816/ecogen79399.

[19] A. Rane and S. J. Joshi. (2021). "Biodecolorization and Biodegradation of Dyes: A Review". *The Open Biotechnology Journal.* **15** (1): 97-108. 10.2174/1874070702115010097.

[20] M. Fraga-Corral, P. Garcia-Oliveira, A. G. Pereira, C. Lourenco-Lopes, C. Jimenez-Lopez, M. A. Prieto, and J. Simal-Gandara. (2020). "Technological Application of Tannin-Based Extracts". *Molecules.* **25** (3). 10.3390/molecules25030614.

[21] N. Li, Q. Wang, J. Zhou, S. Li, J. Liu, and H. Chen. (2022). "Insight into the Progress on Natural Dyes: Sources, Structural Features, Health Effects, Challenges, and Potential". *Molecules.* **27** (10). 10.3390/molecules27103291.

[22] S. Sunariyati, S. Suatma, and Y. Miranda. (2019). "Efforts to Improve Scientific Attitude and Preservation of Local Culture through Ethnobiology-Based Biological Practicum". *Edusains.* **11** (2): 255-263. 10.15408/es.v11i2.13622.

[23] R. Noor, N. Y. Tika, and A. Agustina. (2021). "Preparat jaringan tumbuhan dengan menggunakan pewarna alami sebagai media belajar jaringan tumbuhan praktikum biologi sel". *Jurnal Lentera Pusat Penelitian LPPM UM Metro.* **5** (2): 136-148. 10.24127/jlpp.v5i2.1547.

[24] V. Seithtanabutara, N. Chumwangwapee, A. Suksri, and T. Wongwuttanasatian. (2023). "Potential investigation of combined natural dye pigments extracted from ivy gourd leaves, black glutinous rice and turmeric for dye-sensitised solar cell". *Heliyon.* **9** (11): e21533. 10.1016/j.heliyon.2023.e21533.

[25] S. Yadav, K. S. Tiwari, C. Gupta, M. K. Tiwari, A. Khan, and S. P. Sonkar. (2023). "A brief review on natural dyes, pigments: Recent advances and future perspectives". *Results in Chemistry.* **5**. 10.1016/j.rechem.2022.100733.

[26] L. Chungkrang, S. Bhuyan, and A. R. Phukan. (2021). "Natural Dyes: Extraction and Applications". *International Journal of Current Microbiology and Applied Sciences.* **10** (01): 1669-1677. 10.20546/ijcmas.2021.1001.195.

[27] M. M. Rahman, M. Kim, K. Youm, S. Kumar, J. Koh, and K. H. Hong. (2023). "Sustainable one-bath natural dyeing of cotton fabric using turmeric root extract and chitosan biomordant". *Journal of Cleaner Production.* **382**. 10.1016/j.jclepro.2022.135303.

[28] K. B. Erande, P. Y. Hawaldar, S. R. Suryawanshi, B. M. Babar, A. A. Mohite, H. D. Shelke, S. V. Nipane, and U. T. Pawar. (2021). "Extraction of natural dye (specifically anthocyanin) from pomegranate fruit source and their subsequent use in DSSC". *Materials Today: Proceedings.* **43** : 2716-2720. 10.1016/j.matpr.2020.06.357.

[29] B. Arjun Kumar, G. Ramalingam, D. Karthigaimuthu, T. Elangovan, and V. Vetrivelan. (2022). "Fabrication of natural dye sensitized solar cell using tridax procumbens leaf and beetroot extract mixer as a sensitizer". *Materials Today: Proceedings.* **49** : 2541-2545. 10.1016/j.matpr.2021.04.221.

[30] M. N. Singh, R. Srivastava, and D. I. Yadav. (2021). "Study of different varietis of carrot and its benefits for human health: A review". *Journal of Pharmacognosy and Phytochemistry.* **10** (1): 1293-1299. 10.22271/phyto.2021.v10.i1r.13529.

[31] S. P. Moulick, F. Jahan, M. B. Islam, M. A. Bashera, M. S. Hasan, M. J. Islam, S. Ahmed, D. Karmakar, F. Ahmed, T. Saha, S. S. Dey, F. Boby, M. Saha, B. K. Saha, and M. N. H. Bhuiyan. (2023). "Nutritional

characteristics and antiradical activity of turmeric (Curcuma longa L.), beetroot (Beta vulgaris L.), and carrot (Daucus carota L.) grown in Bangladesh". *Heliyon.* **9** (11): e21495. 10.1016/j.heliyon.2023.e21495.

[32] H. Wagiyanti and R. Noor. (2017). "Red dragon fruit (Hylocereus costaricensis Britt. Et R.) peel extract as a natural dye alternative in microscopic observation of plant tissues: The practical guide in senior high school". *JPBI (Jurnal Pendidikan Biologi Indonesia).* **3** (3): 232-237. 10.22219/jpbi.v3i3.4843.

[33] D. Pintać, K. Bekvalac, N. Mimica-Dukić, M. Rašeta, N. Anđelić, M. Lesjak, and D. Orčić. (2022). "Comparison study between popular brands of coffee, tea and red wine regarding polyphenols content and antioxidant activity". *Food Chemistry Advances.* **1**. 10.1016/j.focha.2022.100030.

[34] A. Haji and M. Rahimi. (2020). "RSM Optimization of Wool Dyeing withBerberis ThunbergiiDC Leaves as a New Source of Natural Dye". *Journal of Natural Fibers.* **19** (8): 2785-2798. 10.1080/15440478.2020.1821293.

[35] Z. Omerogullari Basyigit, C. Eyupoglu, S. Eyupoglu, and N. Merdan. (2023). "Investigation and feed-forward neural network-based estimation of dyeing properties of air plasma treated wool fabric dyed with natural dye obtained from Hibiscus sabdariffa". *Coloration Technology.* **139** (4): 441-453. 10.1111/cote.12665.

[36] M. N. Bukhari, M. A. Wani, M. Fatima, J. S. S. Bukhari, M. Shabbir, L. J. Rather, and F. Mohammad. (2023). "Dyeing of Wool with Sappan Wood Natural Dye Using Metal Salts for Enhancement in Color and Fastness Properties". *Journal of Natural Fibers.* **20** (2). 10.1080/15440478.2023.2208890.

[37] Z. Romdhani, N. Sakji, and M. Hamdaoui. (2022). "Eco-Friendly Dyeing of Wool Fabrics with Natural Dye Extracted from Citrus Sinensis L Peels". *Fibers and Polymers.* **23** (6): 1621-1630. 10.1007/s12221-022-4478-4.

[38] E. Rahayuningsih, A. Mindaryani, D. T. Adriyanti, L. D. Parthasiwi, H. P Adina, and A. E Dyah. (2020). "Conceptual Design of a Process Plant for the Production of Natural Dye from Merbau (Intsia bijuga) Bark". *IOP Conference Series: Materials Science and Engineering.* **778** (1). 10.1088/1757-899x/778/1/012045.

[39] A. Smeriglio, D. Barreca, E. Bellocco, and D. Trombetta. (2017). "Proanthocyanidins and hydrolysable tannins: occurrence, dietary intake and pharmacological effects". *British Journal of Pharmacology.* **174** (11): 1244-1262. 10.1111/bph.13630.

[40] R. Räisänen, A. Primetta, P. Toukola, S. Fager, and J. Ylänen. (2023). "Biocolourants from onion crop side streams and forest mushroom for regenerated cellulose fibres". *Industrial Crops and Products.* **198**. 10.1016/j.indcrop.2023.116748.

[41] A. K. Das, M. N. Islam, M. O. Faruk, M. Ashaduzzaman, and R. Dungani. (2020). "Review on tannins: Extraction processes, applications and possibilities". *South African Journal of Botany.* **135** : 58-70. 10.1016/j.sajb.2020.08.008.

[42] S. Saxena and A. S. M. Raja. (2014). In: "Roadmap to Sustainable Textiles and Clothing, (Textile Science and Clothing Technology, ch. Chapter 2". 37-80. 10.1007/978-981-287-065-0_2.

[43] S. Gala, S. Sumarno, and M. Mahfud. (2020). "Comparison of microwave and conventional extraction methods for natural dyes in wood waste of mahogany (Swietenia mahagoni)". *Journal of Applied Engineering Science.* **18** (4): 618-623. 10.5937/jaes0-23695.

[44] M. L. R. Liman, M. T. Islam, M. M. Hossain, P. Sarker, and M. R. Repon. (2021). "Environmentally benign dyeing mechanism of knitted cotton fabric with condensed and hydrolyzable tannin derivatives enriched bio-waste extracts". *Environmental Technology & Innovation.* **23**. 10.1016/j.eti.2021.101621.

[45] S. Bahri. (2020). "Ekstraksi Kulit Batang Nangka menggunakan Air untuk Pewarna Alami Tekstil". *Jurnal Teknologi Kimia Unimal.* **8** (2): 73-88. 10.29103/jtku.v8i2.2683.

[46] E. Rahayuningsih, T. Marfitania, T. Marfitania, M. Sapto Pamungkas, M. S. Pamungkas, W. Siti Fatimah, and W. S.

Fatimah. (2022). "Optimization of cotton fabrics dyeing process using various natural dye extracts". *Jurnal Rekayasa Proses.* **16** (1). 10.22146/jrekpros.70397.

[47] Y. Ozogul, Y. Ucar, E. E. Tadesse, N. Rathod, P. Kulawik, M. Trif, T. Esatbeyoglu, and F. Ozogul. (2025). "Tannins for food preservation and human health: A review of current knowledge". *Applied Food Research.* **5** (1). 10.1016/j.afres.2025.100738.

[48] A. Pattiya. (2018). In: "Direct Thermochemical Liquefaction for Energy Applications". 3-28. 10.1016/b978-0-08-101029-7.00001-1.

[49] L. Wang, H. Ren, S. Zhai, and H. Zhai. (2021). "Anatomy and cell wall ultrastructure of sunflower stalk rind". *Journal of Wood Science.* **67** (1). 10.1186/s10086-021-02001-6.

[50] G. S. Girolami, T. B. Rauchfuss, and R. J. Angelici. (1999). "Synthesis and technique in inorganic chemistry: a laboratory manual". Publisher University Science Books.

[51] F. H. Schweingruber and A. Börner. (2018). In: "The Plant Stem, ch. Chapter 2". 3-5. 10.1007/978-3-319-73524-5_2.

[52] D. C. Montgomery. (2012). "Design and Analysis of Experiments". John Wiley & Sons, New York.

[53] K. Sinha, P. D. Saha, and S. Datta. (2012). "Response surface optimization and artificial neural network modeling of microwave assisted natural dye extraction from pomegranate rind". *Industrial Crops and Products.* **37** (1): 408-414. 10.1016/j.indcrop.2011.12.032.

[54] S. Trivedi, V. Belgamwar, K. Wadher, and M. Umekar. (2022). "Development and Validation of a UV Spectrophotometric Method for the Estimation of the Synthesized Lentinan–Congo Red Complex". *Journal of Applied Spectroscopy.* **89** (2): 344-349. 10.1007/s10812-022-01364-y.

[55] K. B. Patel, S. Mukherjee, H. Bhatt, D. Rajani, I. Ahmad, H. Patel, and P. Kumari. (2023). "Synthesis, docking, and biological investigations of new coumarin-piperazine hybrids as potential antibacterial and anticancer agents". *Journal of Molecular Structure.* **1276**. 10.1016/j.molstruc.2022.134755.

[56] Y. Soda and E. Bakker. (2019). "Quantification of Colorimetric Data for Paper-Based Analytical Devices". *ACS Sensors.* **4** (12): 3093-3101. 10.1021/acssensors.9b01802.

[57] Y. Sirisathitkul and S. Kaewareelap. (2021). "Color Analysis of Batik Fabric by Facile Smartphone Colorimetry". *International Journal on Advanced Science, Engineering and Information Technology.* **11** (1): 84-91. 10.18517/ijaseit.11.1.11480.

[58] L. Ciaccheri, B. Adinolfi, A. A. Mencaglia, and A. G. Mignani. (2023). "Smartphone-Enabled Colorimetry". *Sensors (Basel).* **23** (12). 10.3390/s23125559.

[59] O. F. Fagbohun, J. P. M. Hui, J. Zhang, G. Jiao, and H. P. V. Rupasinghe. (2024). "Application of response surface methodology and artificial neural network to optimize the extraction of saponins and polyphenols from North Atlantic sea cucumber". *Food Chemistry Advances.* **5**. 10.1016/j.focha.2024.100748.

[60] Luftinor, N. Herlina, and A. Santika Kurniati. (2020). "Coffee bean skin waste extraction for silk dyeing". *IOP Conference Series: Materials Science and Engineering.* **801** (1). 10.1088/1757-899x/801/1/012075.

[61] M. M. Hassan. (2024). "Valorisation of sulphonated lignin as a dye for the sustainable colouration of wool fabric using sustainable mordanting agents: enhanced colour yield, colourfastness, and functional properties". *RSC Sustainability.* **2** (3): 676-685. 10.1039/d3su00402c.

[62] K. Liao, L. Han, Z. Yang, Y. Huang, S. Du, Q. Lyu, Z. Shi, and S. Shi. (2022). "A novel in-situ quantitative profiling approach for visualizing changes in lignin and cellulose by stained micrographs". *Carbohydrate Polymers.* **297** : 119997. 10.1016/j.carbpol.2022.119997.

[63] J. N. Chakraborty and J. N. Chakraborty. (2015)." Fundamentals and Practices in Colouration of Textiles. 10.1201/b18243.

[64] M. Tehrani, F. S. Ghaheh, Z. T. Beni, and M. Rahimi. (2023). "Extracted dyes' stability as

obtained from spent coffee grounds on silk fabrics using eco-friendly mordants". *Environmental Science and Pollution Research.* **30** (26): 68625-68635. 10.1007/s11356-023-27157-0.

[65] A. Darmawan, Widowati, A. Riyadi, H. Muhtar, Kartono, and S. Adhy. (2024). "Enhancing cotton fabric dyeing: Optimizing Mordanting with natural dyes and citric acid". *International Journal of Biological Macromolecules.* **276** (Pt 2): 134017. 10.1016/j.ijbiomac.2024.134017.

[66] D. W. Lestari, V. Atika, Y. Satria, A. Fitriani, and T. Susanto. (2020). "Aplikasi Mordan Tanin pada Pewarnaan Kain Batik Katun Menggunakan Warna Alam Tingi (Ceriops tagal)". *Jurnal Rekayasa Proses.* **14** (2). 10.22146/jrekpros.57891.

[67] Ö. E. İşmal and L. Yıldırım. (2019). In: "The Impact and Prospects of Green Chemistry for Textile Technology". 57-82. 10.1016/b978-0-08-102491-1.00003-4.

[68] J. M. Jabar, T. E. Adedayo, and Y. A. Odusote. (2021). "Green, eco-friendly and sustainable alternative in dyeing cotton fabric using aqueous extract Mucuna slonaei F dye: effects of metal salts pre-mordanting on color strength and fastness properties". *Current Research in Green and Sustainable Chemistry.* **4**. 10.1016/j.crgsc.2021.100151.

[69] S. Ningsih and T. Harmawan. (2022). "Pengaruh Penambahan Al2(SO4)3 Terhadap Derajat Keasaman Air Baku pada Perusahaan Daerah Air Minum (PDAM) Tirta Keumueneng Langsa". *QUIMICA: Jurnal Kimia Sains dan Terapan.* **4** (1): 20-23. 10.33059/jq.v4i1.4317.

[70] M. Dakhem, F. Ghanati, M. Afshar Mohammadian, and M. Sharifi. (2022). "Tea leaves, efficient biosorbent for removal of Al3+ from drinking water". *International Journal of Environmental Science and Technology.* **19** (11): 10985-10998. 10.1007/s13762-022-04313-6.

[71] S. Wan, Z. Ma, Y. Xue, M. Ma, S. Xu, L. Qian, and Q. Zhang. (2014). "Sorption of Lead(II), Cadmium(II), and Copper(II) Ions from Aqueous Solutions Using Tea Waste". *Industrial & Engineering Chemistry Research.* **53** (9): 3629-3635. 10.1021/ie402510s.

[72] H. P. S. Abdul Khalil, A. F. I. Yusra, A. H. Bhat, and M. Jawaid. (2010). "Cell wall ultrastructure, anatomy, lignin distribution, and chemical composition of Malaysian cultivated kenaf fiber". *Industrial Crops and Products.* **31** (1): 113-121. 10.1016/j.indcrop.2009.09.008.

[73] N. Ain, S. A. Sarah, N. Azmi, A. Bujang, and S. R. Ab Mutalib. (2023). "Response surface methodology (RSM) identifies the lowest amount of chicken plasma protein (CPP) in surimi-based products with optimum protein solubility, cohesiveness, and whiteness". *CyTA - Journal of Food.* **21** (1): 646-655. 10.1080/19476337.2023.2272627.

[74] D. J. Cosgrove. (2005). "Growth of the plant cell wall". *Nature Reviews Molecular Cell Biology.* **6** (11): 850-61. 10.1038/nrm1746.

[75] A. O. Özdemir, B. Caglar, O. Çubuk, F. Coldur, M. Kuzucu, E. K. Guner, B. Doğan, S. Caglar, and K. V. Özdokur. (2022). "Facile synthesis of TiO2-coated cotton fabric and its versatile applications in photocatalysis, pH sensor and antibacterial activities". *Materials Chemistry and Physics.* **287**. 10.1016/j.matchemphys.2022.126342.

[76] P. H. F. Pereira, S. A. Costa, S. M. Costa, and V. Arantes. (2025). "Efficient production of lignin nanoparticle colloids and their feasibility for eco-friendly dyeing of natural and synthetic textile fabrics". *Industrial Crops and Products.* **225**. 10.1016/j.indcrop.2024.120390.

[77] S. Liu, W. Ji, T. Wu, Y. He, Y. Huang, Y. Yu, and W. Yu. (2024). "Unraveling the Intricate Interaction: Bonding Mechanism between Tannic Acid and Wood Fibers". *ACS Sustainable Chemistry & Engineering.* **12** (10): 4224-4235. 10.1021/acssuschemeng.3c08010.

[78] A. Lisý, A. Ház, R. Nadányi, M. Jablonský, and I. Šurina. (2022). "About Hydrophobicity of Lignin: A Review of Selected Chemical Methods for Lignin Valorisation in Biopolymer Production". *Energies.* **15** (17). 10.3390/en15176213.

[79] Z. Yu and Z. Yang. (2020). "Understanding different regulatory mechanisms of proteinaceous and non-proteinaceous amino acid formation in tea (Camellia sinensis) provides new insights into the safe and effective alteration of tea flavor and function". *Critical Reviews in Food Science and Nutrition.* **60** (5): 844-858. 10.1080/10408398.2018.1552245.